Journal of Materials Chemistry C

Accepted Manuscript

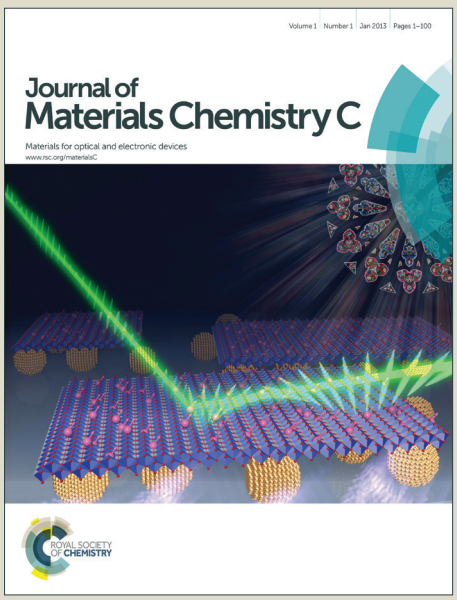

ROYAL SOCIETY OF CHEMISTRY

www.rsc.org/materialsC

Journal Name

RSCPublishing

ARTICLE

Luminescent lanthanide barcodes based on postsynthetic modified nanoscale metal-organic frameworks

Ye Lu, Bing Yan*

Cite this: DOI: 10.1039/x0xx00000x

Received 00th January 2014,
Accepted 00th January 2014

DOI: 10.1039/x0xx00000x

www.rsc.org/

A new method for luminescent barcode based on nanoscale MOFs (MOF-253) is displayed, which the barcoding is realized by postsynthetic method (PSM) to introduce lanthanide ion (Eu^{3+}, Tb^{3+} and Sm^{3+}). The framework does not preferentially include either lanthanide ion, and then any desired lanthanide composition in the result product can be achieved by controlling the stoichiometry of the reactant. The emission intensity of each of lanthanide ion is proportional to its amount in the MOF, resulting in unique luminescent barcodes that depend on the lanthanide ion ratios and compositions.The synthesized barcoded material is successfully applied in marking functional ionic liquid and preparing luminescent thin film.

Introduction

Barcoded material has been achieved considerable attention as labels for multiplexed assays in biological species and anticounterfeiting application.[1] An ideal barcoded material must meet some requirement: it should be stable and available in large scale, its synthesis method should be simple and highly reproducible, its spectral signature should be easily acquired and unique interpreted.[2] Many encoding strategies have been proposed for barcoded materials, including incorporation of segmented nanowires[3] and photopatterning,[4] as well as the use of photonic crystals,[9] conjugated polymer,[7] fluorescent silica colloids,[8] alumina[9] and semiconductor quantum dots (QDs).[10] But some flaw still remains, for example, although QDs or silica colloids barcoded materials have size-dependent multispectral emissions and superior photostability, their preparation with well-defined size is difficult and complicated;[7a, 10d, 11] the emission of QDs or organic polymer generally is broad band which is prone to be overlapped.[12]

Recently, a new conceptual approach have been reported by White and coworker, which is luminescent barcoded systems based on metal-organic frameworks (MOFs) that contain multiple near-IR emitting lanthanides ion as the framework node.[2] Lanthanide ion has inherent advantages on building luminescent barcoded materials, such as sharp emission spectra and various emission bands.[13] In addition, the emission wavelengths of lanthanide ion are fixed and not impacted by environment, not like some organic fluorophores.[14] Moreover, the lanthanide MOFs is able to generate simultaneous emission of several wavelengths using one excitation wavelength for the common antenna; the defined structure of MOFs could determine the precise location of lanthanide ion.[15] But this field still leaves much to be desired. For example, the nanoscale size is important for biomarker and functional thin film;[16] the ligand could have some selectivity to lanthanide ion (as framework node) for different atomic radius so that affect the number and variety of barcode;[2, 17] moreover, the synthesis method should be simplified as far as possible for mass produce.

Postsynthetic method (PSM) maybe is a new choice to solve these problems, whose chemical modification can be performed on the fabricated material rather than on the molecule precursors.[18] Using PSM, the introduction of lanthanide ion could be occurred in fabricated MOFs rather than in precursors. This provides a new possibility for building lanthanide MOFs barcode that barcoding occur on prepared MOFs instead of the process of synthesizing MOFs (Figure 1).

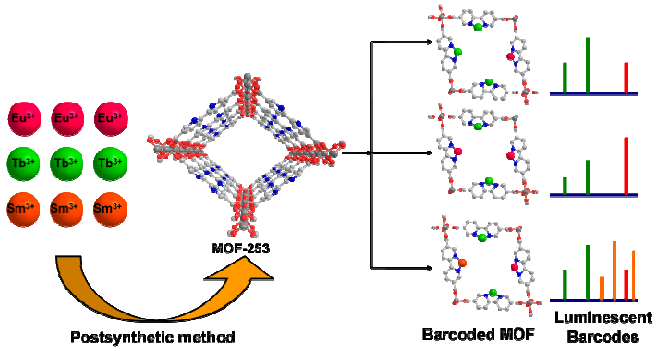

Figure 1 The scheme for luminescent lanthanide barcodes based on PSM.

Herein, we reported a new method for luminescent lanthanide barcode based on postsynthetic modified nanoscale MOFs (MOF-253). Multiple visible emitting lanthanides ion (Eu^{3+}, Tb^{3+} and Sm^{3+}) is introduced to MOF-253 by PSM to realize barcoding. For the nanoscale size, the synthesized barcoded material could be used in marking functional ionic liquid and preparing thin film on ITO glass.

Results and discussion

Preparation of MOF-253-Ln (Ln= Eu, Tb and Sm)

MOF-253 with a bipyridine derivative in the ligand is famous in the inherent advantage of postsynthetic method (PSM).[19] In the structure of MOF-253, a one-dimensional infinite chains of AlO_6

corner-sharing octahedral is built by connecting bpydc (bpydc = 2,2'-bipyridine-5,5'-dicarboxylic) linkers to construct rhombic shaped pores.[19a] The bipyridine group plays two roles, the first is to fix the lanthanide ion, and the second is to sensitize lanthanide ion.[19b] The representative structure of MOF-253 has been isolated by PXRD and a Pawley refinement using the Al(OH)(bpdc) ($bpdc^{2-}$ = 4,4-biphenyldicarboxylate) unit cell parameters in the reported work.[19a, 20] As-synthesized MOF-253 is confirmed by PXRD (Figure S1), elemental analysis (see experiment details), nitrogen adsorption/desorption isotherms (Figure S2) and FT-IR spectroscopy (Figure S3). The corresponding transmission electron microscopy (TEM) image is shown in Figure S4, the size of MOF-253 particles is almost less than 100 nm, although the size distribution is not very satisfactory. MOF-253-Ln is prepared by introducing Ln^{3+} ion (Ln = Eu, Tb and Sm) to MOF-253 through PSM. For reacting completely, the amount of MOF-253 slightly exceed to lanthanide ion, and then the molar ratio of Al^{3+}/Eu^{3+} ion in MOF-253-Eu is really very close to feed ratio, which is determined by inductively coupled plasma (ICP) analysis (details see ESI). After PSM, the crystallization degree is weakened, but the framework is not ruined (Figure S1). The FT-IR spectroscopy also can prove this point (Figure S3). Meantime, the characteristic absorbance of NO_3^- (1390 cm^{-1}) observed in the FT-IR spectroscopy of MOF-253-Ln explain the existence of nitrate in MOFs after PSM.

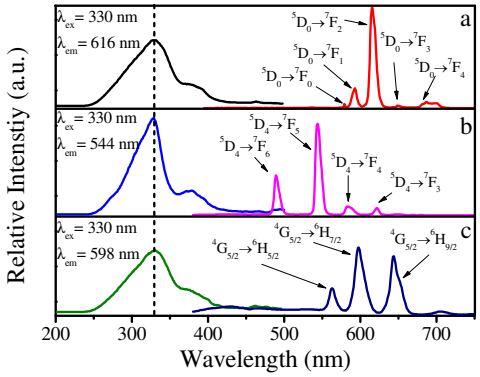

Figure 2 The excitation and emission spectra of MOF-253-Eu (a), MOF-253-Tb (b) and MOF-253-Sm (c)

The emission of MOF-253-Eu exhibit the characteristic transitions of the Eu^{3+} ion at 578, 593, 616, 648 and 687 nm under the excitation of 330 nm, which are ascribed to the $^5D_0 \rightarrow {}^7F_J$ (J = 0-4), transitions, respectively (Figure 2a). The excitation spectrum of MOF-253-Eu is obtained by monitoring the characteristic Eu^{3+} ion emission at 616 nm, which is dominated by a broad band centred at about 330 nm. There is a good match between excitation spectra and UV-visible diffuse reflectance spectrum (DRS) (Figure S5). Similar situation occurs in MOF-253-Tb and MOF-253-Sm. The characteristic Tb^{3+} ion emission could be observed in MOF-253-Tb which is assigned to the $^5D_4 \rightarrow {}^7F_J$ (J = 6, 5, 4 and 3) transitions at 490 nm, 544 nm, 583 nm and 623 nm. The characteristic Sm^{3+} ion emission could also be observed in MOF-253-Sm which is assigned to the $^4G_{5/2} \rightarrow {}^6F_{5/2}$, $^4G_{5/2} \rightarrow {}^6F_{7/2}$ and $^4G_{5/2} \rightarrow {}^6F_{9/2}$ transitions at 562nm, 598 nm and 643 nm. The excitation spectrum of MOF-253-Tb and MOF-253-Sm is similar with MOF-253-Eu, which is obtained by monitoring the characteristic Tb^{3+} ion emission at 544 nm and Sm^{3+} ion emission at 598 nm. The excitation spectra of MOF-253-Ln are all obtained a broad band centred at about 330 nm because of the same sensitizing ligand, bipyridine. This endows MOF-253-based barcoded materials with the same maximum excitation wavelength, whatever the lanthanide ion is. Meantime, the broad excitation band is also solidly proved the coordination effect between lanthanide ion and bipyridine for antenna effect. There is a shoulder band at about 380 nm in the excitation spectra of MOF-253-Ln. This is due to the luminescence of matrix. The excitation spectra of MOF-253 are obtained by monitoring the emission at 550 nm and are dominated by a broad band centred at about 380 nm, and the emission of MOF-253 display broad band centred at about 525-625 nm under excitation at 380 nm (Figure S6). Using MOF-253 as the luminescent centre, the emission of MOF-253 could be clearly observed in the luminescent spectra of MOF-253-Ln, which obtained by exciting MOF-253-Ln at 380 nm (Figure S7).

The lifetime of $^5D_0$ (Eu^{3+}) for MOF-253-Eu, $^5D_4$ (Tb^{3+}) for MOF-253-Tb and $^4G_{5/2}$ (Sm^{3+}) for MOF-253-Sm is 347.47 μs, 122.29 μs and 20.76 μs, respectively, which is shown in the Figure S8 and listed in the Table S1. The MOF-253-Ln also displays satisfactory photostability. The integrated intensity loss of $^5D_0 \rightarrow {}^7F_2$ transitions for MOF-253-Eu, $^5D_4 \rightarrow {}^7F_5$ transitions for MOF-253-Tb and $^4G_{5/2} \rightarrow {}^6F_{7/2}$ transitions for MOF-253-Sm is only 8.21 %, 8.28 % and 8.86 %, respectively, after 24 hrs exposure under UV (λ = 365 nm) (Figure S9).

Preparation of MOF-253-Tb_xEu_{1-x}

After successfully introducing lanthanide ion to MOF-253, we use the same method to yield barcoded MOF-253 with varying Tb^{3+} ion and Eu^{3+} ion stoichiometries: MOF-253-$Tb_{0.99}Eu_{0.01}$, MOF-253-$Tb_{0.995}Eu_{0.005}$ and MOF-253-$Tb_{0.999}Eu_{0.001}$ (see experiment details). The lanthanide compositions in the resulting products were determined by ICP, and directly correlated to the feed ratio of each lanthanide salt (Table S2). This result indicates that the MOF structure does not preferentially include either lanthanide ion, and then any desired lanthanide composition in the result product can be achieved by controlling the stoichiometry of the reactant.

Luminescence studies demonstrate the different lanthanide compositions could result in unique and discernible barcoded signals. The emission of MOF-253-Tb_xEu_{1-x} displays the characteristic transition of Eu^{3+} ion and Tb^{3+} ion with excitation at 330 nm (Figure 3a). With an increase in the amount of Eu^{3+} ion and a decrease in the amount of Tb^{3+} ion, their characteristic emission intensities increase and decree accordingly. That means we can quantitatively control the luminescent intensities of the two emitting lanthanide ion by controlling the lanthanide composition. A plot of the ratio of the integrated intensities of the transition of $^5D_0 \rightarrow {}^7F_2$ (Eu^{3+} ion) and the transition of $^5D_4 \rightarrow {}^7F_5$ (Tb^{3+} ion) reveals a linear relationship between 1: 99 and 0.1: 99.9 Eu^{3+}/Tb^{3+} (molar ratio) (Figure S10). Their relative intensities could be reflected as unique and visible colour which is corresponding with three distinct barcodes. The points of emission of MOF-253-$Tb_{0.95}Eu_{0.05}$, MOF-253-$Tb_{0.99}Eu_{0.01}$ and MOF-253-$Tb_{0.995}Eu_{0.005}$ in CIE chromaticity diagram is green (X = 0.2876, Y = 0.4915), yellow (X = 0.3630 Y = 0.4698) and red (X = 0.5276 Y = 0.3980), respectively (Figure 3b).

Under such low doping ratio of Eu^{3+} ion, the characteristic emission intensity of Eu^{3+} ion is still satisfied. Except for inherent factor (the emission intensity of Eu^{3+} ion emission is generally stronger than Tb^{3+} ion), there may be some energy transfer from Tb^{3+} ion to Eu^{3+} ion.[22] For further explaining the energy transfer, MOF-253-$Eu_{0.01}$ is prepared which have the same Eu^{3+} content to MOF-253-$Tb_{0.99}Eu_{0.01}$ and have not Tb^{3+} ion. The intensity of characteristic Eu^{3+} emission is obviously enhanced after adding Tb^{3+} ion (Figure S11). This indicates the energy transfer from Tb^{3+} to Eu^{3+}.[23] Meantime, the lifetime of MOF-253-Tb_xEu_{1-x} could also obverse the energy transfer. The $^5D_0$ (Eu^{3+}) and $^5D_4$ (Tb^{3+}) lifetime of MOF-253-Tb_xEu_{1-x} is shown in the Figure S12 and listed in Table S1. The $^5D_0$ (Eu^{3+}) lifetime of MOF-253-$Tb_{0.99}Eu_{0.01}$ is 814.80 μs which is increased by almost 2.5 times in comparison to MOF-253-Eu; meanwhile the $^5D_4$ (Tb^{3+}) lifetime of MOF-253-$Tb_{0.99}Eu_{0.01}$ is 39.07

μs which is plunged by about 70 percent in comparison to MOF-253-Tb. The similar situation also occurs on MOF-253-$Tb_{0.999}Eu_{0.001}$ and MOF-253-$Tb_{0.995}Eu_{0.005}$ (Figure S12 and Table S1). The observed change in lifetimes of the Tb^{3+} and Eu^{3+} emission in MOF-253-Tb_xEu_{1-x}, compared to that of pure Tb^{3+} and Eu^{3+} emission (MOF-253-Tb and MOF-253-Eu), further proves that the energy transfer between Tb^{3+} and Eu^{3+} indeed exists.[24]

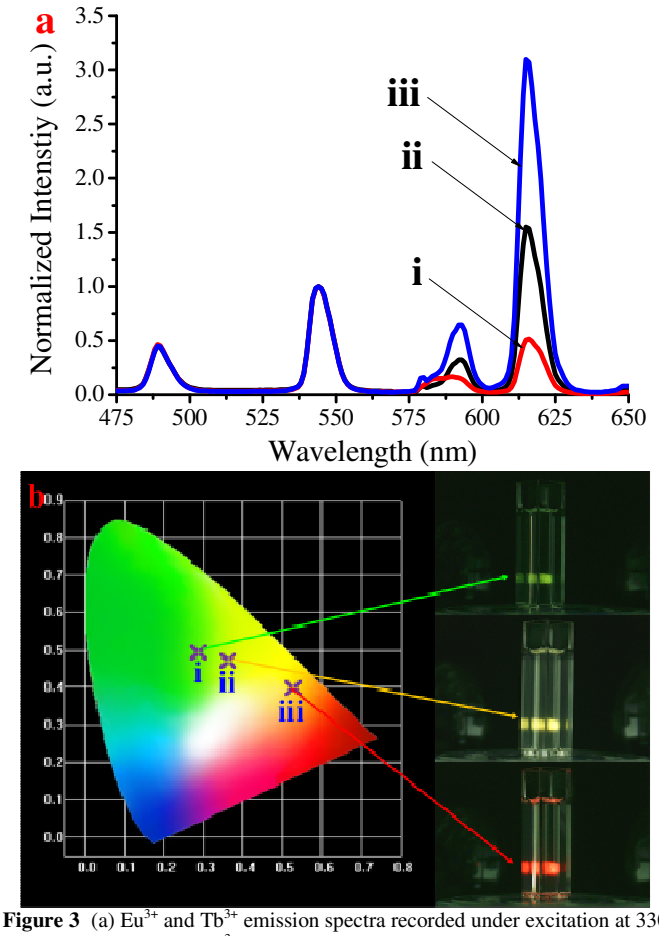

Figure 3 (a) Eu^{3+} and Tb^{3+} emission spectra recorded under excitation at 330 nm, normalized to the Tb^{3+} signal, (b) Color-coded of the barcode readout in CIE chromaticity diagram and the photograph of the MOF-253-based barcoded material (dispersed in ethanol) under excitation at 330 nm, i, ii and iii is MOF-253-$Tb_{0.999}Eu_{0.001}$, MOF-253-$Tb_{0.995}Eu_{0.005}$ and MOF-253-$Tb_{0.99}Eu_{0.01}$, respectively.

The excitation of MOF-253-Tb_xEu_{1-x} is obtained by monitoring the emission at 544 nm (Figure S13a) and 616 nm (Figure S13b). The excitation which monitored Tb^{3+} characteristic emission is similar with MOF-253-Tb. The excitation of matrix (at about 380 nm) could be observed in the excitation which monitored Eu^{3+} characteristic emission. This is due to the low content of Eu^{3+} ion in the MOF. The excitation wavelength of MOF-253 is about 50 nm away from MOF-253-Tb_xEu_{1-x}. So, the emission of MOF-253 would not impact on the barcoded signal.

Preparation of 0.5-MOF-253-Tb_xEu_{1-x}

A comparison experiment has been done for further proving the emission of MOF-253 have no effect to the barcoded signal. The ratio and amount of Ln^{3+} ion is keep the same as before, but the amount of matrix is double. The result product is recorded as 0.5-MOF-253-$Tb_{0.99}Eu_{0.01}$, 0.5-MOF-253-$Tb_{0.995}Eu_{0.005}$ and 0.5-MOF-253-$Tb_{0.999}Eu_{0.001}$. The emission of 0.5-MOF-253-Tb_xEu_{1-x} is the same to MOF-253-Tb_xEu_{1-x} (Figure 4). That means the barcoded signal mainly related with the ratio of different Ln^{3+} ion, not to the matrix. But the increase of matrix directly results the enhancement of the luminescent intensity of matrix in the excitation (Figure S14).

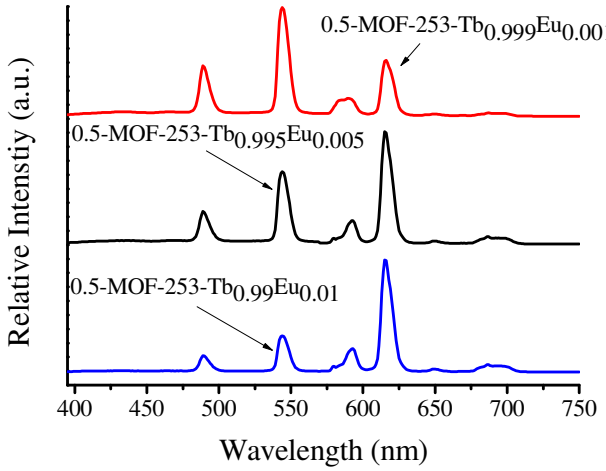

Figure 4 The emission spectra of 0.5-MOF-253-Tb_xEu_{1-x} (λ_{ex} = 330 nm).

Preparation of MOF-253-Ln-1 and MOF-253-Ln-2

For increasing the number and diversity of barcodes, Sm^{3+} ion is introduced to enrich the luminescent signal, and record as MOF-253-Ln-1 and MOF-253-Ln-2 with different stoichiometries of lanthanide ion (see experiment details). The feed ratio of Ln^{3+} ion (Tb^{3+}: Eu^{3+}: Sm^{3+}) is 50: 0.5: 49.5 for MOF-253-Ln-1 and 70: 0.7: 29.3 for MOF-253-Ln-2. The lanthanide compositions in the resulting products are directly correlated to the feed ratio of each lanthanide salt which is determined by ICP (Table S3). The different of atomic radius have not influenced the coordination between lanthanide ion and ligand. The emission spectra of MOF-253-Ln-1 and MOF-253-Ln-2 are normalized to the Eu^{3+} ion signal in Figure 5a, which is obtained by excitation at 330 nm and located at red area in CIE chromaticity diagram (Figure S15). For the same doping ratio of Eu^{3+} ion and Tb^{3+} ion, the emission intensity ratio of Eu^{3+} ion and Tb^{3+} ion is the same in the MOF-253-Ln-1 and MOF-253-Ln-2. This again demonstrates the excellent reproducibility of the barcoded signal based on PSM. With decrease the amount of Sm^{3+} ion, the emission of characteristic Sm^{3+} ion obviously weak from MOF-253-Ln-1 to MOF-253-Ln-2. As expected, it displays a more sophisticated barcode signal from three component lanthanide ion. The excitation of MOF-253-Ln-1 and MOF-253-Ln-2 is obtained by monitoring the characteristic lanthanide ion emission (Figure 5b and 5c). The $^5D_0$ (Eu^{3+}), $^5D_4$ (Tb^{3+}) and $^4G_{5/2}$ (Sm^{3+}) lifetime of MOF-253-Ln-1 is 551.15 μs, 75.38 μs and 31.02 μs, respectively; and the $^5D_0$ (Eu^{3+}), $^5D_4$ (Tb^{3+}) and $^4G_{5/2}$ (Sm^{3+}) lifetime of MOF-253-Ln2 is 613.32 μs, 98.52 μs and 32.89 μs, respectively. Those are all shown in the Figure S16 and listed in the Table S1.

Application of the nanoscale barcoded material based on MOF-253 in functional ion liquid and luminescent thin film

Two systems which have been extensively applied in luminescent material are used to prove the advantage of the nanoscale barcoded material based on MOF-253, one is functional ion liquid, and the other one is ITO glass-supported luminescent thin film.[16, 25] A common ionic liquid, 1-(2-hydroxyethyl)-3-methylimidazolium bromide (IL), is been choose as the matrix to disperse MOF-253-Ln-1, record as IL-MOF-Ln. The synthesis method of IL-MOF-Ln is similar with preparing functional ionic liquid incorporated semiconductor nanoparticle (details see supporting information).[26] The IL-MOF-Ln is clear (about 70 °C) and could emit the luminescent barcoded signal under 330 nm (Figure 6b and 6c). The

luminescent spectra of IL-MOF-Ln are the same to MOF-253-Ln-1 (Figure S17). This means the luminescent barcoded signal is successfully marked on ionic liquid. Meantime, the integrity of MOF-253-Ln-1 is also proved for excitation spectra (Figure S18). ITO glass-supported luminescent thin films of MOF-253-Ln-1 are prepared by direct spin-coating, like the thin films constructed by nanoscale MOF-76.[16] In the photograph, the thin film is transparent (Figure 6d) and emits the luminescent barcoded signal under 330 nm (Figures 6e). From SEM images (Figure 6a), the surface of thin film is continuous and defect-free over a large area. The similarity of emission spectra of the thin film and powder demonstrate the ITO glass have been successfully marked by MOF-253-Ln-1 (Figure S18).

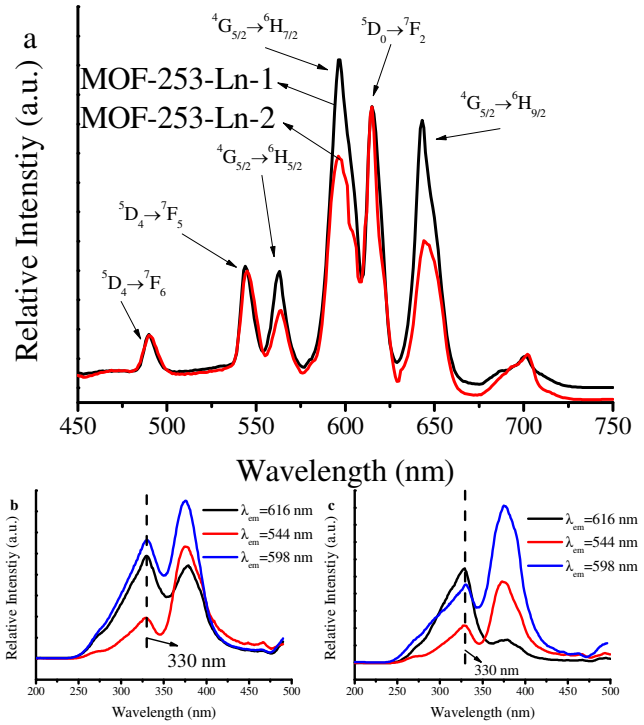

Figure 5 (a) The emission spectra of MOF-253-Ln-1(black) and MOF-253-Ln-2 (red) (λ_{ex} = 330 nm), the excitation spectra of MOF-253-Ln-1 (b) and MOF-253-Ln-2 (c).

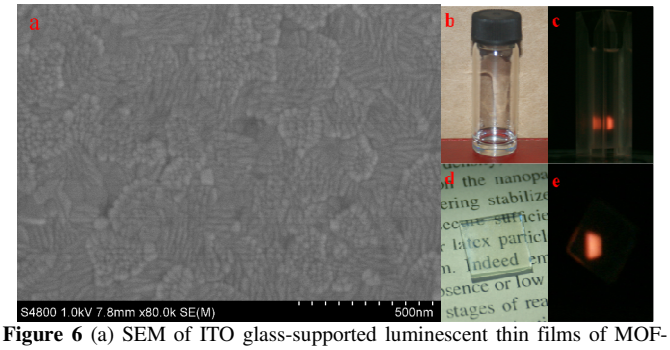

Figure 6 (a) SEM of ITO glass-supported luminescent thin films of MOF-253-Ln-1, the photograph of IL-MOF-Ln (b) and under excitation at 330 nm (c), the photograph of thin film constructed by MOF-253-Ln-1(d) and the red light from the thin film under excitation at 330 nm (e).

Conclusions

In conclusion, we present a new method for luminescent lanthanide barcode based on postsynthetic modified nanoscale MOFs that simultaneously emit several independent visible signals arising from different lanthanide ion. This method is not only simple and straightforward, but also suitable to almost all lanthanide ions. Furthermore, the barcoded materials have be successfully used to mark ionic liquid and prepare spin coating thin film ITO glass. The nanoscale of matrix (MOF-253) endows the barcoded materials with greater advantage in the practical application.

Experiment

Chemicals. Chemicals were purchased from commercial sources. All solvents were analytical grade and without further purification. $Eu(NO_3)_3{\cdot}xH_2O$, $Tb(NO_3)_3{\cdot}xH_2O$ and $Sm(NO_3)_3{\cdot}xH_2O$ were prepared by dissolving oxides (Eu_2O_3, Tb_4O_7 or Sm_2O_3) in concentrated nitric acid (HNO_3).

Physical characterization. The elemental analyses are measured with a Vario ELIII elemental analyser. X-ray diffraction patterns are recorded on a Rigaku D/ max-Rb diffractometer equipped with a Cu anode in a 2θ range from 5 to 45°. Scanning electronic microscope (SEM) was measured on Hitachi S-4800. Transmission electron microscope (TEM) experiments were conducted on a JEOL2011 microscope operated at 200 kV. Nitrogen adsorption/desorption isotherms are measured by using a Nova 1000 analyser under the liquid nitrogen temperature. Luminescence excitation and emission spectra of samples are obtained on Edinburgh FLS920 spectrophotometer. Luminescence lifetime measurements are carried out on an Edinburgh FLS920 phosphorimeter using a microsecond pulse lamp as excitation source. The data of life time is achieved from fitting the experiment luminescent decay. UV-visible diffuse reflectance spectrum was taken with BWS003. The measurement of metal ion was performed on Agilent 7700X inductively coupled plasma-mass spectrometer (ICPMS).

MOF-253. MOF-253 (Al(OH)(bpydc)) is synthesized according to the references.[19a] MOF-253 was prepared from hydrothermal reaction of $AlCl_3{\cdot}6H_2O$ (151 mg, 0.625 mmol), 2,2'-bipyridine-5,5'-dicarboxylic acid (153 mg, 0.625 mmol) and 10 mL N,N'-dimethylformamide (DMF) at 120 °C for 24 hrs. The resulting white microcrystalline powder was then collected with by centrifugation and washed with DMF. The solid products were washed with methanol via Soxhlet extraction for 24 hrs, and then was collected by filtration and finally dried at 200 °C under vacuum for 12 hrs to give [Al(bpydc)(OH)], MOF-253 (165 mg, 90 %). Anal. Calcd for $C_{12}H_7AlN_2O_5$: C, 50.34; H, 2.45; N, 9.79. Found: C, 50.35; H, 2.43; N, 9.78.

MOF-253-Ln (Ln = Eu, Tb and Sm). The preparation of MOF-253-Eu was carried out as follows: The compound Al(OH)(bpydc) (31.7 mg, 0.11 mmol), solution of $Eu(NO_3)_3{\cdot}xH_2O$ in the acetonitrile (10 mL, 10 mmol/L) and acetonitrile (5 mL) were added to a Tefloncapped 20 mL scintillation vial and heated on a hotplate at 65 °C for 24 hrs. The resulting white solid product was washed with acetonitrile by ultrasonic three times and dried at 65 °C under vacuum for 12 hrs to give $(Al(bpydc)(OH)(Eu(NO_3)_3)_{0.91})$, MOF-253-Eu (61.8 mg, 94.5 %). Anal. Calcd. for $C_{12}H_7AlEu_{0.91}N_{4.73}O_{13.19}$: C, 24.01; H, 1.18; N, 11.04. Found: C, 24.00; H, 1.17; N, 11.05. ICP analysis showed that the molar ration of Al^{3+}/Eu^{3+} was 10.99:9.98. MOF-253-Tb and MOF-253-Sm was prepared in a similar manner to MOF-253-Eu.

MOF-253-Tb_xEu_{1-x} (x = 0.99, 0.995 and 0.999). The preparation of MOF-253-$Tb_{0.99}Eu_{0.01}$ was carried out as follows: The compound Al(OH)(bpydc) (31.7 mg, 0.11 mmol), solution of $Tb(NO_3)_3{\cdot}xH_2O$ in the acetonitrile (9.9 mL, 10 mmol/L), $Eu(NO_3)_3{\cdot}xH_2O$ in the

acetonitrile (1 mL, 0.01 mmol/L) and acetonitrile (5 mL) were added to a Tefloncapped 20 mL scintillation vial and heated on a hotplate at 65 °C for 24 hrs. The resulting white solid product was washed with acetonitrile by ultrasonic three times and dried at 65 °C under vacuum for 12 hrs to give $(Al(bpydc)(OH)(Tb(NO_3)_3)_{0.91}(Eu(NO_3)_3)_{0.009})$, MOF-253-$Tb_{0.99}Eu_{0.01}$ (63mg, 95 %). Anal. Calcd for $C_{12}H_7AlTb_{0.91}Eu_{0.009}N_{4.757}O_{13.271}$: C, 23.90; H, 1.17; N, 11.03. Found: C, 23.89; H, 1.18; N, 11.04. ICP analysis showed that the molar ration of $Al^{3+}/Tb^{3+}/Eu^{3+}$ was 10.99: 9.99: 0.10. MOF-253-$Tb_{0.995}Eu_{0.005}$ and MOF-253-$Tb_{0.999}Eu_{0.001}$ was prepared in a similar manner to MOF-253-$Tb_{0.99}Eu_{0.01}$.

0.5-MOF-253-Tb_xEu_{1-x} (x = 0.99, 0.995 and 0.999). 0.5-MOF-253-Tb_xEu_{1-x} (x = 0.99, 0.995 and 0.999) is prepared by the same method, the amount and ratio of lanthanide ion keep the same as before, but the amount of matrix, MOF-253, is double.

MOF-253-Ln-1 and MOF-253-Ln-2. MOF-253-Ln-1 and MOF-253-Ln-2 is prepared by the same method, except for different ratio of lanthanide ion.

1-(2-Hydroxyethyl)-3-methylimidazolium bromide (IL). IL is synthesized according to the references.[27] Toluene as a solvent, the 1-mythylimidazole was mixed with bromoethanol (1:1 equiv.); the mixture was stirred at 110 °C for 24 hrs under nitrogen atmosphere. Then, the pale-yellow viscous product was washed with ethyl acetate at least 3 times. Yield: 90 %. ^{1}H NMR δ (ppm in D-DMSO): 9.19(s 1H), 7.71(s 1H), 7.74(s 1H), 4.32(t 2H), 3.88(s 3H), 3.72(t 2H).

IL-MOF-253-Ln. The MOF-253-Ln-1 powder (0.6 g) was added to the ionic liquid (6 g) in a round-bottomed flask at room temperature, and the reaction mixture was heated at 120 ^{0}C and vigorously stirred for 4 h in an argon atmosphere. The resulting mixture was stand under 120 ^{0}C overnight to deposit the solid. The IL would gradually become the solid in room temperature (Figure S19), so the deposition should be taken under 120 °C. The clear liquid is extracted while it is hot.

Spin coating thin film. MOF-253-Ln-1 powder was dispersed in DMF. The concentration was in the range of 10-25 mg/mL. The suspension was then centrifuged at 2000 rpm for 10 min to remove big particles before it was spun onto a precleaned 1 cm × 1 cm ITO glass. A Laurell spin-coater was used and the spin rate was 1000 rpm for 60 s. The solvent adsorbed was removed by heating films at 100 ºC for 12 hrs under vacuum after spin-coating.

Notes and references

Department of Chemistry, Tongji University, Shanghai 200092, P. R. China. Fax: (+86) 21-65982287; E-mail: byan@tongji.edu.cn

† Electronic Supplementary Information (ESI) available: Experimental, synthesis and characterization details. See DOI: 10.1039/b000000x/

1. (*a*) D. C. Pregibon, M. Toner and P. S. Doyle, *Science*, 2007, **315**, 1393; (*b*) J. Wang, *J. Mater. Chem.*, 2008, **18**, 4017; (*c*) S. R. Nicewarner-Pena, R. G. Freeman, B. D. Reiss, L. He, D. J. Pena, I. D. Walton, R. Cromer, C. D. Keating and M. J. Natan, *Science*, 2001, **294**, 137; (*d*) B. J. Battersby, G. A. Lawrie, A. P. R. Johnston and M. Trau, *Chem. Commun.*, 2002, 1435.
2. K. A. White, D. A. Chengelis, K. A. Gogick, J. Stehman, N. L. Rosi and S. Petoud, *J. Am. Chem. Soc.*, 2009, **131**, 18069.
3. (*a*) D. H. Park, Y. K. Hong, E. H. Cho, M. S. Kim, D. C. Kim, J. Bang, J. Kim and J. Joo, *ACS Nano*, 2010, **4**, 5155; (*b*) R. L. Stoermer, J. A. Sioss and C. D. Keating, *Chem. Mater.* 2005, **17**, 4356.
4. E. Fernandez-Rosas, R. Gomez, E. Ibanez, L. Barrios, M. Duch, J. Esteve, C. Nogues and J. A. Plaza, *Small*, 2009, **5**, 2433.
5. F. Cunin, T. A. Schmedake, J. R. Link, Y. Y. Li, J. Koh, S. N. Bhatia and M. J. Sailor, *Nat. Mater.*, 2002, **1**, 39.
6. X. L. Feng, G. M. Yang, L. B. Liu, F. T. Lv, Q. Yang, S. Wang and D. B. Zhu, *Adv. Mater.*, 2012, **24**, 637.
7. (*a*) F. Ramiro-Manzano, R. Fenollosa, E. Xifre-Perez, M. Garin and F. Meseguer, *Adv Mater.*, 2011, **23,** 3022; (*b*) A. P. R. Johnston, B. J. Battersby, G. A. Lawrie and M. Trau, *Chem. Commun.*, 2005, 848.
9. A. Santos, V. S. Balderrama, M. Alba, P. Formentin, J. Ferre-Borrull, J. Pallares and L. F. Marsal, *Adv. Mater.*, 2012, **24**, 1050.
10. (*a*) G. Wang, Y. K. Leng, H. J. Dou, L. Wang, W. W. Li, X. B. Wang, K. Sun, L. S. Shen, X. L. Yuan, J. Y. Li, K. Sun, J. S. Han, H. S. Xiao and Y. Li, *Acs Nano*, 2013, **7**, 471; (*b*) X. B. Wang, G. Wang, W. W. Li, B. X. Zhao, B. Xing, Y. K. Leng, H. J. Dou, K. Sun, L. S. Shen, X. L. Yuan, J. Y. Li, K. Sun, J. S. Han, H. S. Xiao, Y. Li, P. Huang and X. Y. Chen, *Small*, 2013, **9**, 3327; (*c*) Y. L. Gao, W. L. Stanford and W. C. W. Chan, *Small*, 2011, *7*, 137; (*d*) Y. J. Zhao, H. C. Shum, H. S. Chen, L. L. A. Adams, Z. Z. Gu and D. A. Weitz, *J. Am. Chem. Soc.*, 2011, **133**, 8790; (*e*) S. Rauf, A. Glidle and J. M. Cooper, *Chem. Commun.*, 2010, **46**, 2814.
11. I. L. Medintz, A. R. Clapp, H. Mattoussi, E. R. Goldman, B. Fisher and J. M. Mauro, *Nat. Mater.*, 2003, **2**, 630.
12. (*a*) A. J. Nozik, M. C. Beard, J. M. Luther, M. Law, R. J. Ellingson and J. C. Johnson, *Chem. Rev.*, 2010, **110**, 6873; (*b*) D. T. McQuade, A. E. Pullen and T. M. Swager, *Chem. Rev.*, 2000, **100**, 2537.
13. (*a*) J. Feng and H. J. Zhang, *Chem. Soc. Rev.*, 2013, **42**, 387; (*b*) K. Binnemans, *Chem. Rev.*, 2009, **109**, 4283; (*c*) B. Yan, *RSC Adv.*, 2012, **2**, 9304.
14. (*a*) S. V. Eliseeva and J. C. G. Bunzli, *Chem. Soc. Rev.*, 2010, **39**, 189; (*b*) L. D. Carlos, R. A. Ferreira, Z. Bermudez Vde and S. J. Ribeiro, *Adv. Mater.*, 2009, **21**, 509; (*c*) J. Rocha, L. D. Carlos, F. A. A. Paz and D. Ananias, *Chem. Soc. Rev.*, 2011, **40**, 926.
15. Y. J. Cui, Y. F. Yue, G. D. Qian and B. L. Chen, *Chem. Rev.*, 2012, **112**, 1126.
16. H. L. Guo, Y. Z. Zhu, S. L. Qiu, J. A. Lercher and H. J. Zhang, *Adv. Mater.*, 2010, **22**, 4190.
17. M. Li, D. Li, M. O'Keeffe and O. M. Yaghi, *Chem. Re*v., 2014, **114**, 1343.
18. S. M. Cohen, *Chem. Rev.*, 2012, **112**, 970.
19. (*a*) E. D. Bloch, D. Britt, C. Lee, C. J. Doonan, F. J. Uribe-Romo, H. Furukawa, J. R. Long and O. M. Yaghi, *J. Am. Chem. Soc.*, 2010, **132**, 14382; (*b*) Y. Lu and B. Yan, *J. Mater. Chem. C*, 2014, **2**, 5526.
20. I. Senkovska, F. Hoffmann, M. Froba, J. Getzschmann, W. Bohlmann, S. Kaskel, *Micropor. Mesopor. Mater.*, 2009, **122**, 93.
22. (*a*) Y. J. Cui, H. Xu, Y. F. Yue, Z. Y. Guo, J. C. Yu, Z. X. Chen, J. K. Gao, Y. Yang, G. D. Qian and B. L. Chen, *J. Am. Chem. Soc.*, 2012, **134**, 3979; (*b*) X. T. Rao, T. Song, J. K. Gao, Y. J. Cui, Y. Yang, C. D. Wu, B. L. Chen and G. D. Qian, *J. Am. Chem. Soc.*, 2013, **135**, 15559.
23. T. S. Atabaev, H. K. Kim and Y. H. Hwang, *J. Colloid. Interf. Sci.*, 2012, **373**, 14.
24. C. J. Gao, A. M. Kirillov, W. Dou, X. L. Tang, L. L. Liu, X. H. Yan, Y. J. Xie, P. X. Zang, W. S. Liu and Y. Tang, *Inorg. Chem.*, 2014, **53**, 935.
25. (*a*) K. Binnemans, *Chem. Rev.*, 2007, **107**, 2592.
26. B. Rodriguez-Cabo, E. Rodil, H. Rodriguez, A. Soto and A. Arce, *Angew. Chem. Int. Edit.*, 2012, **51**, 1424.
27. (*a*) J. R. Harjani, J. Farrell, M. T. Garcia, R. D. Singer and P. J. Scammells, *Green Chem.*, 2009, **11**, 821; (*b*) Y. Mei, Y. Lu and B. Yan, *New J. Chem.*, 2013, **37**, 2619.

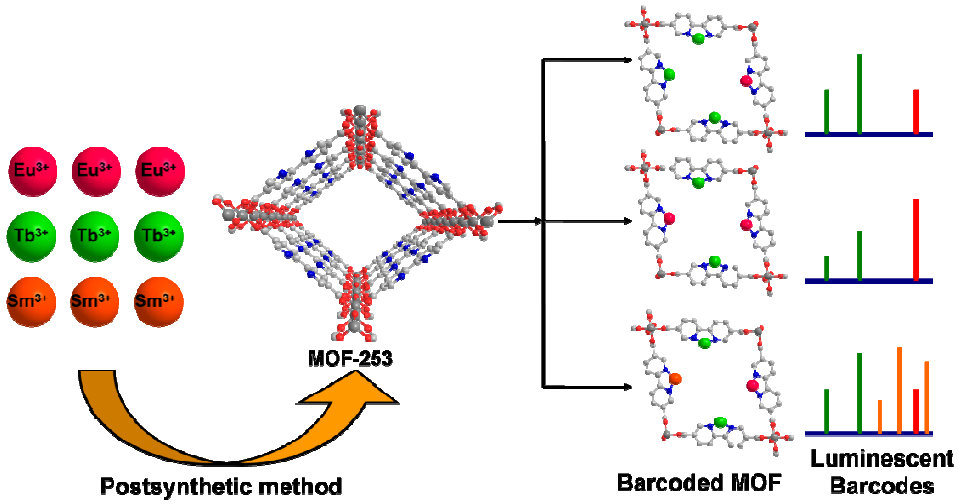

A new method for luminescent barcode based on nanoscale MOFs (MOF-253) is displayed, which the bacrcoding is realized by postsynthetic method (PSM) to introduce lanthanide ion (Eu^{3+}, Tb^{3+} and Sm^{3+}). The synthesized barcoded material is successfully applied in marking functional ionic liquid and preparing luminescent thin film.